

# Poly(L-lactic acid)/Silicone Dioxide Nanocomposites Prepared via *In Situ* Melt Polycondensation of L-Lactic Acid in the Presence of Acidic Silica Sol: Dispersion Stability of Nanoparticles During Dehydration/Oligomerization

Zhaoqin Ma, Linbo Wu, Bo Peng

Department of Chemical & Biological Engineering, State Key Laboratory of Chemical Engineering, Zhejiang University, Hangzhou 310027, China

Received 14 August 2010; accepted 1 December 2010

DOI 10.1002/app.33876

Published online 29 November 2011 in Wiley Online Library (wileyonlinelibrary.com).

**ABSTRACT:** In this work, the stability of nanoparticles during the dehydration/oligomerization (D/O) stage *in situ* melt polycondensation of L-lactic acid to prepare poly(L-lactic acid) (PLLA)/SiO<sub>2</sub> nanocomposite was studied. The change in the appearance of the reaction mixture was tracked, and the resultant oligo(L-lactic acid) (OLLA)/SiO<sub>2</sub> and PLLA/SiO<sub>2</sub> nanocomposites were characterized by transmission electron microscopy, <sup>1</sup>H-NMR, and light transmittance. The electric double layer and the grafted OLLA chains provided static and steric stabilities during the early and late phases, respectively. However, there existed an intermediate transitional phase with weak stability when the static stability was weakened, but sufficient steric stability had not yet been established; this led

to soft or hard aggregation, depending on the SiO<sub>2</sub> loading and agitation conditions. At low or moderate SiO<sub>2</sub> loading (<5–10%), the soft aggregation could be depressed with appropriate agitation conditions and redispersed with the aid of gradually established steric interaction energy. Consequently, well-dispersed PLLA/SiO<sub>2</sub> nanocomposites with SiO<sub>2</sub> loadings of 5 and 10% were successfully prepared by *in situ* melt polycondensation with an arc stirrer at 400 and 600 rpm, respectively, during the D/O stage. © 2011 Wiley Periodicals, Inc. *J Appl Polym Sci* 124: 3980–3987, 2012

**Key words:** biodegradable; nanocomposites; polycondensation; stabilization

## INTRODUCTION

Poly(L-lactic acid) (PLLA) is an important biobased and biodegradable polymer having reasonably good properties and tremendous market potential in packing materials, fibers, agricultural films, biomaterials, and so on.<sup>1–3</sup> Because of its slow crystallization rate and large crystalline size, its mechanical properties and heat and impact resistances are not good enough for some demanding applications,<sup>4–6</sup> and therefore, it is often modified by means of copolymerization,<sup>7</sup> blending,<sup>8</sup> nanocompositing,<sup>9–13</sup> and so on. PLLA nanocomposites often possess much better properties if the nanoparticles are well-dispersed

and appropriate interfacial interaction is established.<sup>9,10,14–16</sup>

In previous studies, we reported an *in situ* melt polycondensation with acidic silica sol (aSS; SiO<sub>2</sub> nanoparticles dispersed in water) to prepare PLLA/SiO<sub>2</sub> nanocomposites<sup>17</sup> and found that the SiO<sub>2</sub> nanoparticles acted as nucleating agents and, therefore, promoted the crystallization of PLLA.<sup>18</sup> In the *in situ* melt polycondensation process, ultrasound was used to prevent aggregation of SiO<sub>2</sub> nanoparticles and to enhance the dispersion stability during dehydration/oligomerization (D/O).<sup>17</sup> However, it is technically difficult and uneconomic to use ultrasound in large-scale production from the viewpoint of engineering. So, it is necessary to understand the stability mechanism better, to solve the problem of dispersion stability in the D/O stage, and thus, to establish a practical *in situ* melt polycondensation to prepare PLLA/SiO<sub>2</sub> nanocomposites.

In this study, the effects of the stirrer type and speed and temperature on the dispersion stability at various SiO<sub>2</sub> loadings during the D/O stage were investigated experimentally, and a mechanism of dispersion stability of the nanoparticles is presented. We found that the soft aggregation could be

Correspondence to: L. Wu (wulinbo@zju.edu.cn).

Contract grant sponsor: National Nature Science Foundation of China; contract grant numbers: 20406018, 20304012 and 20674067.

Contract grant sponsor: National Basic Research Program of China (973 Program); contract grant number: 2011CB606004.

depressed with appropriate agitation and the nanoparticles could be redispersed with the aid of gradually established steric interaction energy at low to moderate SiO<sub>2</sub> loadings ( $\phi_{\text{SiO}_2} \leq 10\%$ ).

## EXPERIMENTAL

### Materials

L-Lactic acid (LLA) aqueous solution (90 wt %, optical purity = 98%) was supplied by Musashino Chemical Corp. (Nanchang, China). aSS (25.4 wt % SiO<sub>2</sub> nanoparticles, average diameter = 11.7 nm) was purchased from Zhejiang Yuda Chemical Co. (Shangyu, China). Stannous chloride (SnCl<sub>2</sub>·2H<sub>2</sub>O) and toluene-*p*-sulfonic acid (TSA; Shanghai, China) were purchased from Shanghai Chemical Reagent Co. (Shanghai, China) and were used without further purification.

### Reaction procedure

#### D/O

An aqueous solution of LLA, aSS [5, 10, and 20 wt %  $\phi_{\text{SiO}_2}$  based on LLA], and TSA (0.28 wt % based on LLA) were charged into a 250-mL, four-necked flask equipped with a mechanical stirrer. The reaction mixture was gradually heated to 130°C in 1 h under stirring at 10<sup>4</sup> Pa and dehydrated/oligomerized at 130°C/10<sup>4</sup> Pa for about 2 h. Then, a reflux condensing tube was mounted to the flask, the temperature was raised to 150°C, the pressure was reduced to 400 Pa gradually in about 20 min, and the reaction mixture was further dehydrated/oligomerized at 150°C/400 Pa for another 3 h. The side product, L-lactide, was refluxed at 83°C in the condensing tube. During the D/O stage, the change in the appearance of the reaction mixture was observed directly, and samples were taken from the reactor at predetermined times, and pictures were taken when they were cooled to room temperature (RT). At the end of the D/O stage, the resultant oligo(L-lactic acid) (OLLA)/SiO<sub>2</sub> nanocomposite was poured out, and the residue gel adhered to the reactor wall and stirrer was roughly determined gravimetrically.

#### Melt polycondensation

The resultant OLLA/SiO<sub>2</sub> nanocomposite was further melt-polycondensed after the addition of SnCl<sub>2</sub>·2H<sub>2</sub>O (0.4 wt % based on OLLA). It was heated to 180°C, and the pressure was reduced gradually to 400 Pa in about 30 min. The reaction was continued at 180°C/400 Pa for 4 h.

### Characterization

#### Transmission electron microscopy (TEM)

TEM (JEOL JEMACRO-1230, Japan) was used to directly observe the dispersion of SiO<sub>2</sub> nanoparticles

in the nanocomposites (OLLA/SiO<sub>2</sub> and PLLA/SiO<sub>2</sub>). A specimen with a thickness of 80 nm was microtomed at RT with an ultramicrotome with a diamond knife. The ultrathin slice was then supported by a copper grid for TEM observation.

#### Light transmittance

The light transmittance of the OLLA/SiO<sub>2</sub> nanocomposite was used to characterize the dispersion of SiO<sub>2</sub> nanoparticles indirectly as it decreased with the formation of aggregation. A nanocomposite was dissolved/dispersed in chloroform at a concentration of 1 wt % and then spun-coated on a glass slide substrate with a spin coater (KW-4A, Institute of Microelectronics of Chinese Academy of Sciences, Beijing, China) at 1000 rpm for 15 s and then at 2500 rpm for 30 s. After the film was dried *in vacuo* at 45°C for over 12 h to remove the residual chloroform, the light transmittance of the film was measured with an ultraviolet-visible light spectrophotometer [UV-2800(A)/2802/2802S] at wavelengths of 400–800 nm. The transmittance of the glass slide was assumed to be 100%.

#### <sup>1</sup>H-NMR

<sup>1</sup>H-NMR was used to determine the chain length of the oligomer in the matrix (OLLA) and on the surface of the SiO<sub>2</sub> nanoparticles [(g-OLLA) the nanoparticles were grafted with oligo(L-lactic acid)]. The posttreatment of the OLLA/SiO<sub>2</sub> nanocomposite to obtain OLLA and g-OLLA samples was the same as previously reported,<sup>17</sup> except that the precipitation procedure was not used. The <sup>1</sup>H-NMR characterization was carried out with a Bruker Avance DMX 500 (500 MHz, Switzerland) with CDCl<sub>3</sub> as the solvent and 0.03 vol % TMS (Tetramethylsilane) as the internal standard. The polymerization degree ( $X_n$ ) was calculated from the area of the chemical shifts of —OCH(CH<sub>3</sub>)CO— at 5.19 ppm ( $S_{5.2}$ ) and HOCH(CH<sub>3</sub>)— at 4.20 ppm ( $S_{4.2}$ ), see eq. (1):<sup>19</sup>

$$X_n = S_{5.2}/S_{4.2} + 1 \quad (1)$$

## RESULTS

### Instability during D/O

In the melt polycondensation of LLA, LLA is often dehydrated and oligomerized in the absence of catalyst, and then, the resultant oligomer is melt-polycondensed in the presence of a binary catalyst, SnCl<sub>2</sub>/TSA, to produce PLLA. Recently, we presented a modified D/O method in the presence of TSA (i.e., only the Sn catalyst was added at the melt polycondensation stage).<sup>20</sup> It resulted in a largely shortened D/O time and greatly enhanced the polymerization degree of the oligomer and was also

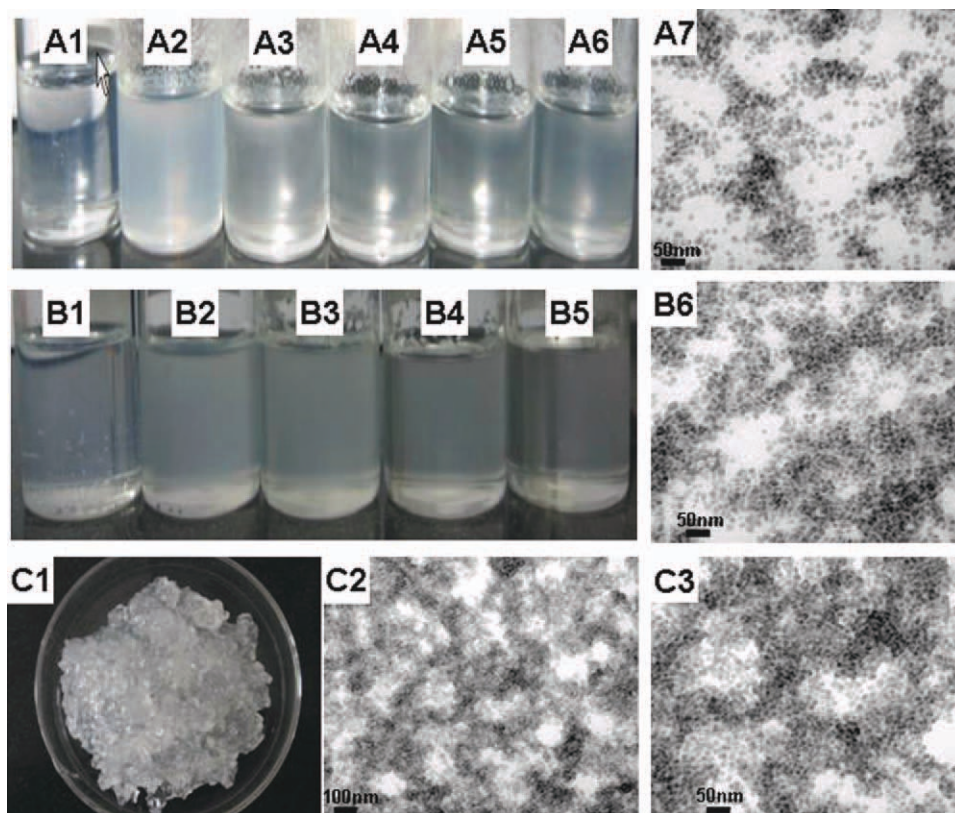


**Figure 1** Appearances (A1–A6, B1–B5, and C1, pictures taken at RT) of the reaction mixtures during the D/O stage and the TEM micrographs (A7, B6, and C2–C3) of OLLA/SiO<sub>2</sub> nanocomposites prepared at SiO<sub>2</sub> loadings of (A) 5, (B) 10, and (C) 20% (paddle stirrer, 200 rpm): A1, starting material; A2, 100°C/10<sup>4</sup> Pa, 40 min; A3–A6, 130°C/10<sup>4</sup> Pa, 60, 100, 140, and 180 min, respectively; B1, starting material; B2, 100°C/10<sup>4</sup> Pa, 40 min; B3–B5, 130°C/10<sup>4</sup> Pa, 60, 100, and 140 min, respectively; and C1, 100°C/10<sup>4</sup> Pa, 40 min. [Color figure can be viewed in the online issue, which is available at [wileyonlinelibrary.com](http://wileyonlinelibrary.com).]

beneficial to molecular weight growth during melt polycondensation.<sup>20</sup> This new catalyst addition policy was also used in the *in situ* melt polycondensation of LLA in this study.

In the *in situ* melt polycondensation of LLA in the presence of silica sol, the dispersion of the silica nanoparticles became unstable to a certain extent during the D/O stage whether the traditional<sup>17</sup> or modified D/O method<sup>20</sup> was used. Typically, the clear reaction mixture of aqueous LLA and silica sol became turbid after most free water was removed; this indicated that a unstable or metastable state

appeared. The reaction mixture then gradually recovered back to translucent (or transparent at low SiO<sub>2</sub> loading), but aggregation of the nanoparticles in the oligomers was still observed by TEM. The extent of instability depended on the SiO<sub>2</sub> loading. Figure 1 shows the appearances of the reaction mixtures during the D/O stage. (All the pictures were taken at RT, and the mixture at reaction temperature was more turbid by comparison.) However, the appearance at RT reflected the change trend at the reaction temperature (the effect of temperature is discussed in a later section), and we prepared TEM

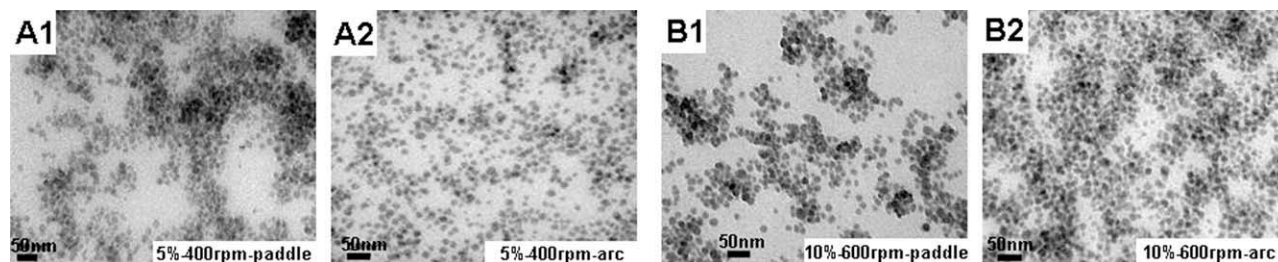


**Figure 2** TEM micrographs of the OLLA/SiO<sub>2</sub> nanocomposites prepared with paddle and arc stirrers under the indicated conditions.

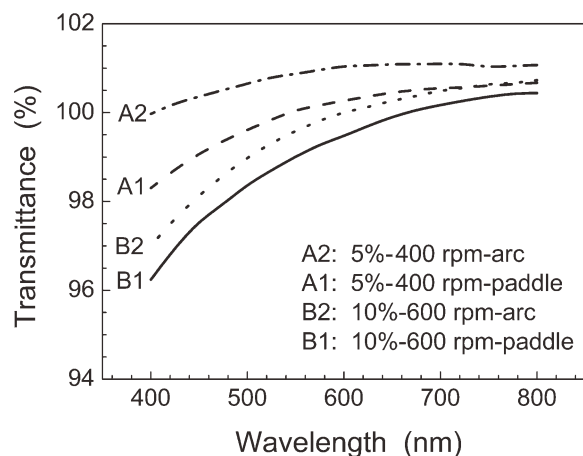


**Figure 3** Light transmittance of the OLLA/SiO<sub>2</sub> nanocomposite films prepared with paddle and arc stirrers under the indicated conditions.

micrographs of SiO<sub>2</sub> nanoparticles in the oligomers prepared at 5–20% SiO<sub>2</sub> loading using a paddle stirrer at 200 rpm. At a SiO<sub>2</sub> loading of less than 5 wt %, only a slight unstable phenomenon was observed. When the SiO<sub>2</sub> loading increased to 10 wt %, the aggregation of nanoparticles aggravated, and some gel-like substance formed at the reactor wall. At a SiO<sub>2</sub> loading of 20 wt %, most of the reaction mixture became a gel-like product.

As reported in our previous article, the aggregated nanoparticles could be redispersed with the aid of ultrasound, but it is technically difficult and uneconomical to use ultrasound in large-scale production. So, it is necessary to enhance the stability in the *in situ* D/O stage in a facile and cheap way and, thus, to prepare PLLA/SiO<sub>2</sub> nanocomposites via *in situ* melt polycondensation.

#### Effect of stirrer type on stability

In this study, we found that stirring played an important role in the stability.

When an arc stirrer was used instead of a paddle one, the stability clearly improved. The TEM micrographs shown in Figure 2 indicate that there was clear aggregation in the OLLA/SiO<sub>2</sub> nanocomposites prepared by the paddle stirrer, whereas the nanoparticles in the nanocomposites prepared by the arc stirrer showed improved dispersion. The higher light transmittance of the nanocomposite films illustrated in Figure 3 confirmed less aggregation and improved dispersion. In addition, the use of the arc stirrer was also helpful for preventing gel formation effectively, as shown in Table I.

#### Effect of stirring speed on stability

The effect of stirring speed on the stability was studied further with the arc stirrer, and the results are

**TABLE I**  
Content of Gel ( $\phi_{\text{gel}}$ ) Formed During D/O with Paddle (Data in Parenthesis) and Arc Stirrers at Various SiO<sub>2</sub> Loadings and Stirring Speeds (N's)

$\phi_{\text{SiO}_2}$ (%)	N (rpm)	$\phi_{\text{gel}}$ (%)
5	200	~ 0
	400	~ 0 (~ 0)
	600	~ 0
	900	~ 0
10	200	~ 20
	400	~ 10
	600	~ 0 (~ 10)
	900	~ 0
20	900	~ 50 (~ 90)
	1300	~ 30

shown in Figures 4 and 5 and Table I. The effect depended on the SiO<sub>2</sub> loading. At a lower SiO<sub>2</sub> loading of 5%, the effect of stirring speed was relatively small. There was no clear gel formed at stirring speeds of 200–900 rpm, and the light transmittance of the nanocomposite films increased slightly with stirring speed, being as high as 99.7–101.3%. The TEM micrographs indicated that the best dispersion of nanoparticles was achieved at a stirring speed of 400 rpm. Lower or higher stirring speeds led to uneven dispersion or certain aggregation.

At a moderate SiO<sub>2</sub> loading of 10%, the effect of stirring speed was obvious. At a slow stirring speed of 200 rpm, about 20% gel was formed, a clear aggregation was formed [Fig. 5, B1], and the light transmittance ranged from 94.1 to 99.5%. With increasing stirring speed, the gel content decreased, and the dispersion of nanoparticles and transmittance of the OLLA/SiO<sub>2</sub> nanocomposites improved gradually. At a stirring speed of 600 rpm, no gel was formed. The nanoparticles were evenly dispersed, and the nanocomposite had a light

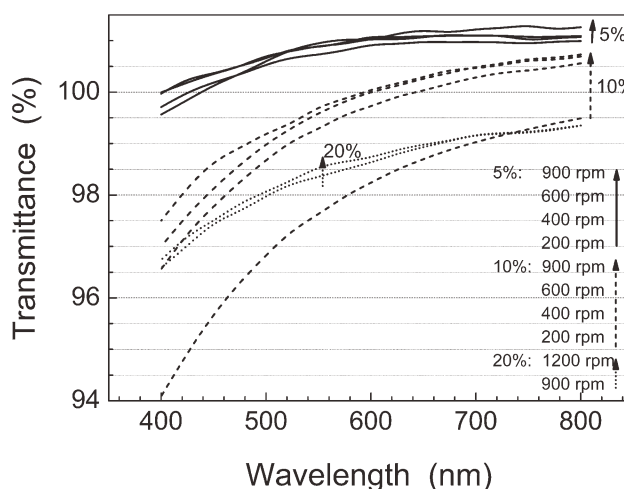


**Figure 4** Light transmittance of the OLLA/SiO<sub>2</sub> nanocomposite films prepared with an arc stirrer at various stirring speeds.

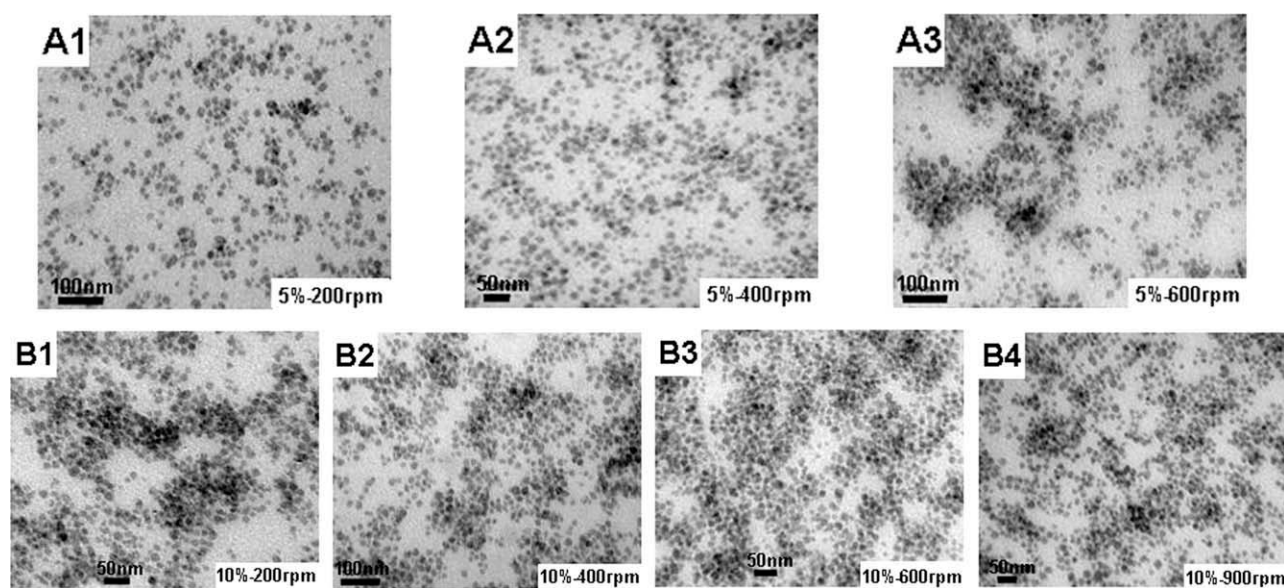


**Figure 5** TEM micrographs of the OLLA/SiO<sub>2</sub> nanocomposites prepared with an arc stirrer under the indicated conditions.

transmittance as high as 97.0–100.7%. At a higher stirring speed of 900 rpm, the dispersion and transmittance remained almost unchanged.

At a high SiO<sub>2</sub> loading of 20%, the reaction mixture was very prone to gelling, even when a high stirring speed was used. The gel content decreased with increasing stirring speed, but the formation of gel could not be eliminated, even at very high speeds, and the high loading resulted in low light transmittance (96.6–99.3%) in the nanocomposite films.

#### Improvement of stability

From the previous results, it can be seen that it was impracticable to achieve good stability and dispersion at a high SiO<sub>2</sub> loading of 20% under ordinary conditions, but it was facile to achieve good stability and dispersion at a low to moderate loading by the selection of the appropriate stirrer type and stirring speed: arc stirrer at 400 rpm for 5% SiO<sub>2</sub> loading

and at 600 rpm for 10% SiO<sub>2</sub> loading. Under these conditions, the reaction mixture showed clearly improved stability during the D/O stage, and PLLA/SiO<sub>2</sub> nanocomposites with nanoscale well-dispersed SiO<sub>2</sub> particles were successfully prepared, as shown in Figure 6.

#### DISCUSSION

In aSS, the SiO<sub>2</sub> nanoparticles were evenly dispersed in acidic aqueous medium and stabilized by an electric double layer (EDL) mechanism.<sup>21–23</sup> When they were mixed with LLA aqueous solution, the EDL [Fig. 7(A)] and the stability remained as the new medium, water + LLA, had similarly strong polarity, acidity, and hydrophilicity.

After oligomerization, the nanoparticles were grafted with oligomers (denoted as g-OLLA) via reactions of Si–OH with the terminal COOH or OH group of LLA or OLLA,<sup>17,24,25</sup> as shown in Figure 7(B). The OLLA in matrix and g-OLLA on the

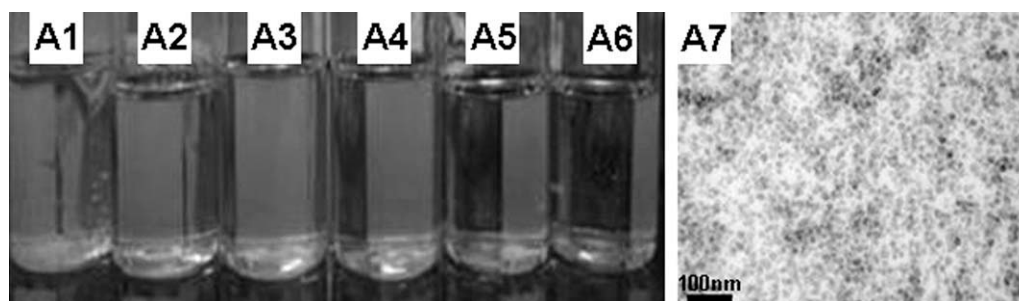


**Figure 6** Appearances (A1–A6, pictures taken at RT) of the reaction mixtures during the D/O stage and the TEM micrograph (A7) of the final PLLA/SiO<sub>2</sub> nanocomposite prepared via *in situ* melt polycondensation ( $\phi_{\text{SiO}_2} = 10\%$ , arc stirrer, 600 rpm; A1, starting material; A2, 100°C/10<sup>4</sup> Pa, 40 min; A3–A6, 130°C/10<sup>4</sup> Pa, 60, 100, 140, and 180 min, respectively).

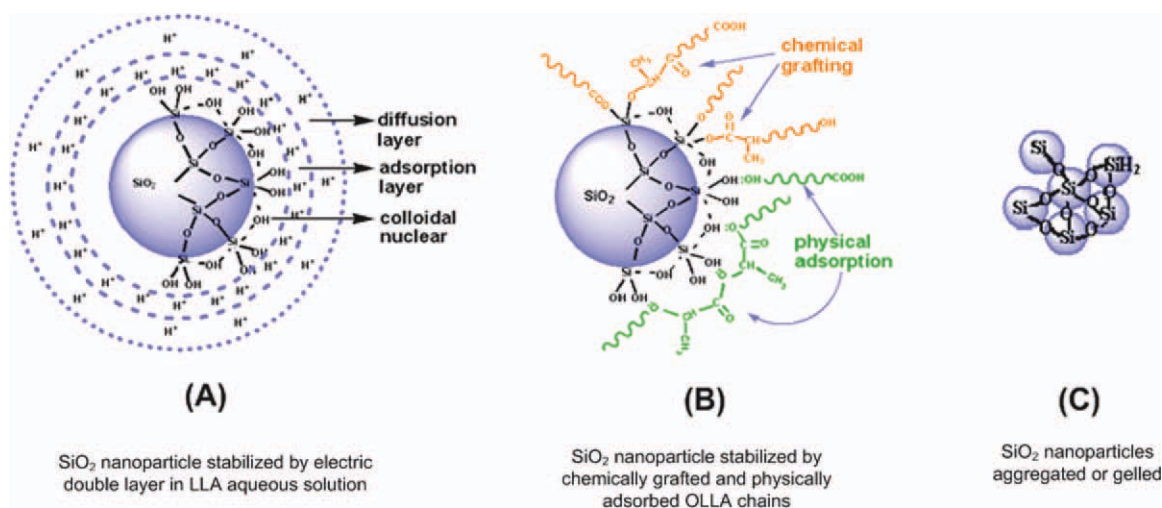


**Figure 7** Schematic diagrams of the three different dispersion states of SiO<sub>2</sub> nanoparticles. [Color figure can be viewed in the online issue, which is available at [wileyonlinelibrary.com](http://wileyonlinelibrary.com).]

surface were separated from the sample obtained at the end of oligomerization and were characterized with <sup>1</sup>H-NMR (Fig. 8). Their polymerization degrees calculated from eq. (1) were 8 and 7, respectively. That is, the grafted g-OLLA chains had enough length to provide sufficient steric interaction energy to stabilize the nanoparticles in the OLLA matrix.<sup>26–28</sup> In subsequent reaction, the polymer chains in the polymer matrix and on the surface of nanoparticles grew synchronously, enhancing the steric stability, resulting in similar hydrophobicity and weak polarity in the matrix and on the surface, and therefore, ensuring good nanoscale dispersion of SiO<sub>2</sub> in PLLA.

During the D/O stage, the EDL and grafted chains provided static and steric stabilities during the early and late phases, respectively, as shown in Figure 9. However, the static stability was weakened as the dehydration proceeded. When the free water was almost removed, the EDL was nearly destroyed, but sufficient steric stability was not yet established. The number and length of the chains grafted were not enough to sufficiently stabilize the nanoparticles. Such a transitional phase led to weak stability and the aggregation of nanoparticles, as reflected by the turbid appearance of the reaction mixture.

If the potential energy between nanoparticles fell into the second potential well, the nanoparticles formed reversible soft aggregation, which could be depressed with appropriate external energy input and redispersed through growing steric interaction energy. However, if the potential energy exceeded the potential energy barrier and fell into the first potential well, the nanoparticles formed irreversible hard aggregation or gelation, which could not be redispersed, as illustrated in Figures 7(C) and 9.

Both ultrasound and agitation provide external energy input, but the latter is more practical and economical. Both the stirrer type and stirring speed had an effect on the stability. The arc stirrer was better than the paddle one; this suggests that too strong a shear force may not have been beneficial for the stability. At a given SiO<sub>2</sub> loading, an appropriate stirring speed provided appropriate agitation energy to prevent the nanoparticles from aggregating. However, too high an agitation energy or too strong a shear at higher stirring speed again led to aggregation to a certain extent. The appropriate agitation energy needed to stabilize the nanoparticles depended on the SiO<sub>2</sub> loading. At higher SiO<sub>2</sub> loadings, a higher agitation energy and, therefore, a higher stirring speed were needed. In this study, 400 and 600 rpm appeared appropriate for 5 and 10% SiO<sub>2</sub> loadings.

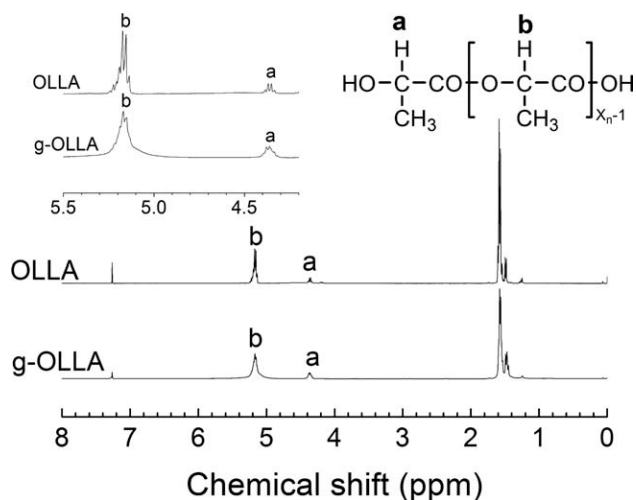


**Figure 8** <sup>1</sup>H-NMR spectra of OLLA and g-OLLA.

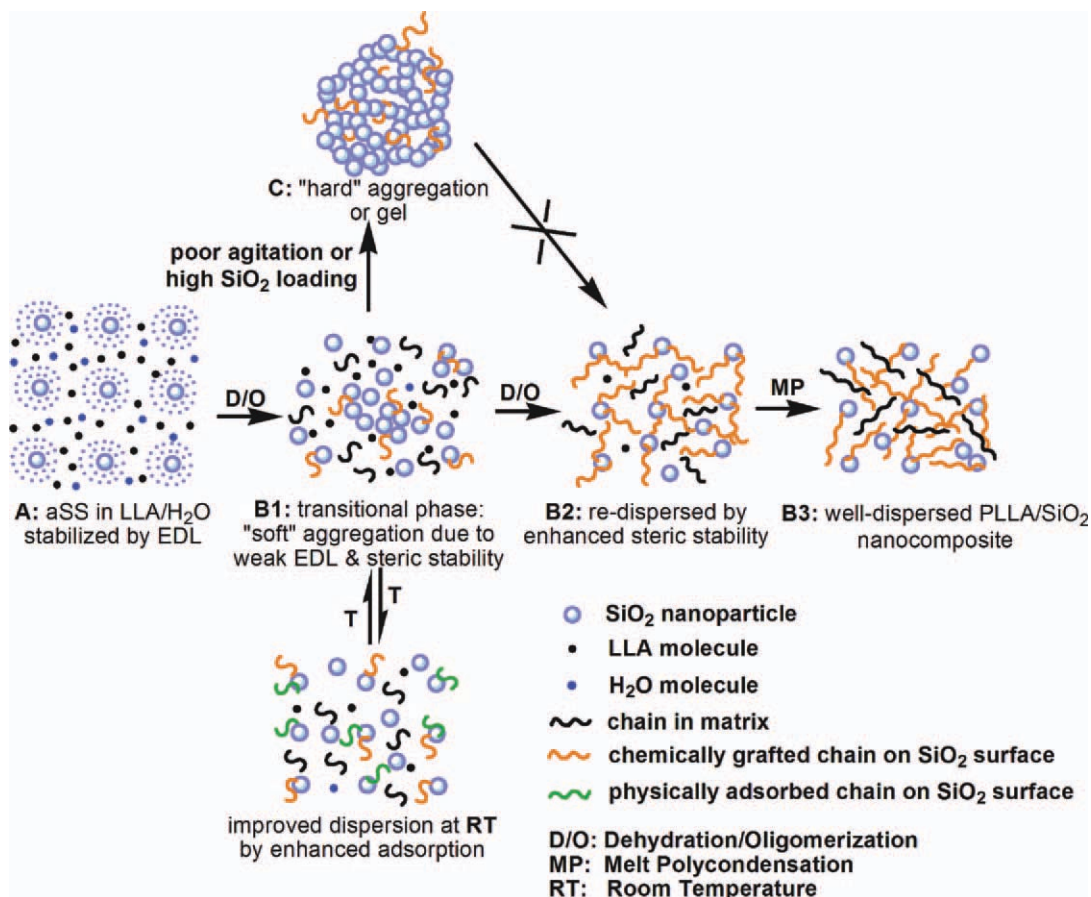


**Figure 9** Schematic diagrams of the evolution of the stability of SiO<sub>2</sub> nanoparticles during *in situ* melt polycondensation. [Color figure can be viewed in the online issue, which is available at [wileyonlinelibrary.com](http://wileyonlinelibrary.com).]

In addition, the temperature seemed to have a certain effect on the stability or at least on the appearance of the reaction mixture, especially during the transitional phase. This was confirmed from observation of the samples at various temperatures. The samples at RT were more transparent [Fig. 10(A), at increasing reaction times from left to right] compared with their true appearance at the reaction temperature, but it did reflect the true change trend. When the samples were heated to 70°C, the samples

became more turbid [Fig. 10(B)]. When the samples were cooled to RT again, the appearance nearly recovered [Fig. 10(C)].

Such an effect may be attributed to the physical adsorption of OLLA chains on the particle surface via hydrogen bonds at RT and desorption at high temperature, as illustrated in Figures 7(B) and 9. At low temperatures, the physically adsorbed chains provided extra steric stability and, therefore, resulted in a more transparent appearance. At high

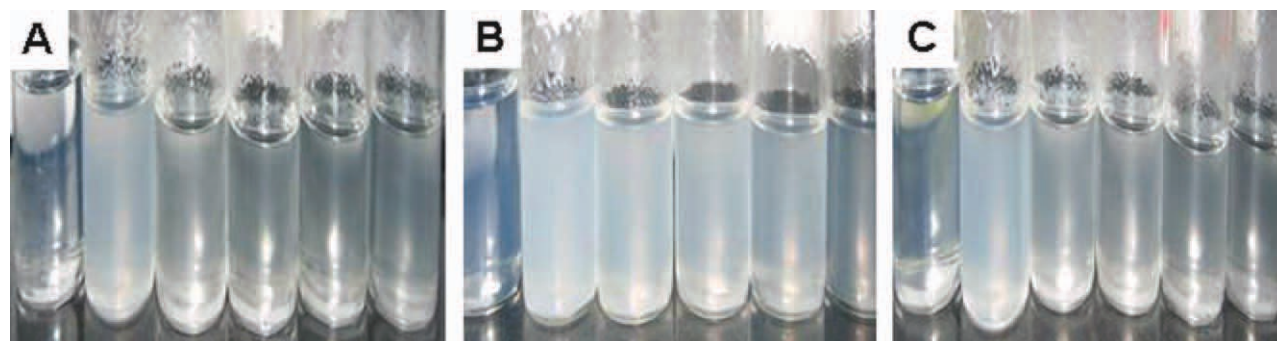


**Figure 10** Appearances of the reaction mixtures at various temperatures: (A) RT, (B) heated to 70°C, and (C) cooled to RT again ( $\phi_{\text{SiO}_2} = 5\%$ ; paddle, 200 rpm). [Color figure can be viewed in the online issue, which is available at [wileyonlinelibrary.com](http://wileyonlinelibrary.com).]

temperatures, the hydrogen bonding was broken, and the chains were desorbed; this led to weakened steric stability and low transparency. As the chemical grafting was still weak at the transitional phase, the temperature dependence of the stability was remarkable. When the chemical grafting was enhanced with reaction time, the effect of temperature was weakened gradually.

### CONCLUSIONS

The stability of nanoparticles during the D/O stage in the *in situ* melt polycondensation of LLA to prepare PLLA/SiO<sub>2</sub> nanocomposite was studied in this work. The EDL and the grafted OLLA chains provided static and steric stabilities during the early and late phases, respectively. However, there existed an intermediate transitional phase with weak stability when the static stability was weakened, but sufficient steric stability was not established; this led to soft or hard aggregation, depending on the SiO<sub>2</sub> loading and agitation conditions. At low or moderate SiO<sub>2</sub> loadings ( $\phi_{\text{SiO}_2} < 5\text{--}10\%$ ), the soft aggregation could be depressed with appropriate agitation conditions, and the nanoparticles could be redispersed with the aid of gradually established steric interaction energy, which resulted from growing grafted chains. The appropriate agitation energy to stabilize the nanoparticles depended on the SiO<sub>2</sub> loading. Well-dispersed PLLA/SiO<sub>2</sub> nanocomposites with 5 and 10% SiO<sub>2</sub> loadings were successfully prepared via *in situ* melt polycondensation with an arc stirrer at 400 and 600 rpm, respectively, in the D/O stage. However, at high SiO<sub>2</sub> loadings ( $\phi_{\text{SiO}_2} \geq 20\%$ ) or under improper agitation conditions, the nanoparticles were prone to form hard aggregation or gels that could not be redispersed.

### References

1. Drumright, R. E.; Gruber, P. R.; Henton, D. E. *Adv Mater* 2000, 12, 1841.
2. Bendix, D. *Polym Degrad Stab* 1998, 59, 129.
3. Kovalchuk, A.; Fischer, W.; Epple, M. *Macromol Biosci* 2005, 5, 289.
4. Nam, J. Y.; Ray, S. S.; Okamoto, M. *Macromolecules* 2003, 36, 7126.
5. Tsuji, H.; Ikada, Y. *Polymer* 1996, 37, 595.
6. Perego, G.; Cella, G. D.; Bastioli, C. *J Appl Polym Sci* 1996, 59, 37.
7. Jeon, O.; Lee, S. H.; Kim, S. H.; Lee, Y. M.; Kim, Y. H. *Macromolecules* 2003, 36, 5585.
8. Focarete, M. L.; Scandola, M. *Macromolecules* 2002, 35, 8472.
9. Yan, S. F.; Yin, J. B.; Yang, Y.; Dai, Z. Z.; Ma, J.; Chen, X. S. *Polymer* 2007, 48, 1688.
10. Thellen, C.; Orroth, C.; Froio, D.; Ziegler, D.; Lucciarini, J.; Farrell, R.; D'souza, N. A.; Ratto, J. A. *Polymer* 2005, 46, 11716.
11. Ray, S. S.; Maiti, P.; Okamoto, M.; Yamada, K.; Ueda, K. *Macromolecules* 2002, 35, 3104.
12. Zhang, D. H.; Kandadai, M. A.; Cech, J.; Roth, S.; Curran, S. A. *J Phys Chem B* 2006, 110, 12910.
13. Deng, X. M.; Hao, J. Y.; Wang, C. S. *Biomaterials* 2001, 22, 2867.
14. Ray, S. S.; Yamada, K.; Ogami, A.; Okamoto, M.; Ueda, K. *Macromol Rapid Commun* 2002, 23, 943.
15. Ray, S. S.; Yamada, K.; Okamoto, M.; Ueda, K. *Polymer* 2003, 44, 857.
16. Paul, M. A.; Alexandre, M.; Degee, P.; Calberg, C.; Jerome, R.; Dubois, P. *Macromol Rapid Commun* 2003, 24, 561.
17. Wu, L. B.; Cao, D.; Huang, Y.; Li, B. G. *Polymer* 2008, 49, 742.
18. Cao, D.; Wu, L. B. *J Appl Polym Sci* 2009, 111, 1045.
19. Espartero, J. L.; Rashkov, I.; Li, S. M.; Manolova, N.; Vert, M. *Macromolecules* 1996, 29, 3535.
20. Song, F. C.; Wu, L. B. *J Appl Polym Sci* 2011, 120, 2780.
21. Xu, G. L.; Zhang, J. J.; Song, G. Z. *Power Technol* 2003, 134, 218.
22. Sadasivan, S.; Rasmussen, D. H.; Chen, F. P.; Kannabiran, R. K. *Colloids Surf A* 1998, 132, 45.
23. Kobayashi, M.; Juillerat, F.; Galletto, P.; Bowen, P.; Borkovec, M. *Langmuir* 2005, 21, 5761.
24. Bikiaris, D.; Karavelidis, V.; Karayannidis, G. *Macromol Rapid Commun* 2006, 27, 1199.
25. Yao, X. Y.; Tian, X. Y.; Xie, D. H.; Zhang, X.; Zheng, K.; Xu, J.; Zhang, G. Z.; Cui, P. *Polymer* 2009, 50, 1251.
26. Shin, Y. C.; Lee, D.; Lee, K.; Ahn, K. H.; Kim, B. *J Ind Eng Chem* 2008, 14, 515.
27. Pham, K. N.; Fullston, D.; Crentsil, K. S. *J Colloid Interface Sci* 2007, 315, 123.
28. Jesionowski, T.; Zurawska, J.; Krysztafkiewicz, A. *J Mater Sci* 2002, 37, 1621.